

REAL-TIME SIMULATIONS OF HIGH-ENERGY NUCLEAR COLLISIONS

ALEX KRASNITZ

UCEH, Universidade do Algarve, P-8000 Faro, Portugal

RAJU VENUGOPALAN

Niels Bohr Institute, Blegdamsvej 17, Copenhagen, Denmark, DK-2100

We discuss real time simulations of high energy nuclear collisions in a classical effective theory of QCD at small x . At high transverse momenta, our results match the lowest order predictions of pQCD based mini-jet calculations. We discuss novel non-perturbative behaviour of the small x modes seen at small transverse momenta.

1 Introduction

The space-time evolution of nuclei in high energy heavy ion collisions and the various proposed signatures of the hot and dense matter formed¹ depend sensitively on the initial conditions for the evolution⁷. These are the distributions of partons in each of the nuclei *prior* to the collision. In the standard perturbative QCD approach, observables from the collision are computed by convolving the known parton distributions of each nucleus with the elementary parton-parton scattering cross sections. At the RHIC and LHC colliders, hundreds of mini-jets may be formed in the initial collision². Final state interactions of these mini-jets are often described in multiple scattering models (see Ref.³ and references therein) or in classical cascade approaches (see Ref.⁴ and references therein). The possible “quenching” of these mini-jets has also been studied and proposed as a signature of the formation of a quark gluon plasma⁵. Recently, initial conditions for the energy density and velocity obtained in the mini-jet approach have been used in a simple hydrodynamic model to study the late time evolution of matter in high energy nuclear collisions⁶.

In this paper, we describe an *ab initio* QCD based approach to the study of high energy nuclear collisions. This model naturally incorporates coherence effects which are important at small x and small transverse momenta and simultaneously reproduces the standard mini-jet results at large transverse momenta. It also contains a self-consistent space-time picture of the nuclear collision. The model is based on an effective action approach to QCD initially developed by McLerran and Venugopalan⁹, and later further developed by Ayala, Jalilian-Marian, McLerran and Venugopalan¹⁰ and by Jalilian-Marian, Kovner, Leonidov and Weigert^{11,12,13}.

The above mentioned effective action contains one dimensionful parameter, μ , the total color charge squared per unit area. The classical fields corresponding to the saddle point solutions of the effective theory are the non-Abelian analogue of the Weizsäcker-Williams fields in electrodynamics. Exact analytical expressions for these fields have been obtained recently^{11,14}. Further, it has been shown explicitly that μ obeys renormalization group equations in rapidity y and momentum transfer squared Q^2 . These reduce to the well known BFKL and DGLAP equations respectively in the appropriate limits^{12,13}.

The above model was applied to the problem of nuclear collisions by Kovner, McLerran and Weigert. They formulated the problem as the collision of Weizsäcker-Williams fields¹⁵. Further, classical gluon radiation corresponding to perturbative modes was studied by these authors and later in greater detail by several others^{16,17,18}. In the small x limit, the classical Yang-Mills result agrees with the quantum Bremsstrahlung result of Gunion and Bertsch²⁰.

The perturbative approach is of course very relevant and useful. However, it is essential to consider the full non-perturbative approach for the following reasons. Firstly, the classical gluon radiation computed perturbatively is infrared singular, as is also the case in mini-jet calculations, and therefore rather sensitive to the cut-off. It was argued in Ref.^{15,17} that a natural scale for the cut-off is $k_t \sim \alpha_S \mu$. However, to be sure, it is important to perform a full calculation. Secondly, the non-perturbative approach is crucial to study the space-time evolution of the nuclei and in particular, the possible thermalization of the system. This has several ramifications for various quark gluon plasma signatures. For instance, if thermalization does occur, then hydrodynamic evolution of the system is reasonable¹⁹. In that event, our approach would provide the necessary initial temperature and velocity profiles for such an evolution⁶.

We discuss in this paper first results from real time simulations of the full, non-perturbative evolution of classical non-Abelian Weizsäcker-Williams fields. Such a simulation is possible since the fields are classical. Similar classical simulations have been performed in the context of sphaleron induced baryon number violation²³ and chirality violating transitions in hot gauge theories²⁴. In brief, the idea is as follows²¹. We write down the lattice Hamiltonian which describes the evolution of the small x classical gauge fields. It is the Kogut-Susskind Hamiltonian in 2+1-dimensions coupled to an adjoint scalar field. The lattice equations of motion for the fields are determined straightforwardly. The initial conditions for the evolution are the Weizsäcker-Williams fields for the nuclei before the collision. Interestingly, the dependence on the sources does not enter through the Hamiltonian but instead through the initial conditions.

A related approach is that of Mueller, Kovchegov and Wallon²⁵, where they combined Mueller’s dipole picture of high energy scattering²⁶ with the classical Yang–Mills picture¹⁴ to study nucleon–nucleus scattering. For alternative approaches, we refer the reader to the work of Makhlin and Surdutovich²⁷ and of Balitsky²⁸.

Our paper is organized as follows. In the following section we briefly discuss the problem of initial conditions for nuclear collisions and the perturbative computation of classical gluon production. We also discuss a non-perturbative Hamiltonian approach to the solution of the full Yang-Mills equations. In section 3, we formulate the problem of solving the Yang-Mills equations on the lattice. Starting from the lattice action and assuming boost invariance, we write down the lattice Hamiltonian, the Hamilton equations of motion and the initial conditions for the dynamical fields and their conjugate momenta on the lattice. The initial conditions depend on a single dimensional parameter μ , the color charge per unit area per unit rapidity. Numerical results from our simulations and comparisons to lattice perturbation theory (LPTh) are discussed in section 4. These are performed for a range of values of $\mu = 0.015$ – 0.2 , and for lattice sizes from 10×10 to 160×160 measured in units of the lattice spacing. We summarize our results in section 5.

2 The Weizsäcker–Williams approach to high energy nuclear collisions

The model of McLerran and Venugopalan of gluon fields in a nucleus at small x was applied to nuclear collisions by Kovner, McLerran and Weigert¹⁵. We shall now discuss their formulation of the problem and their perturbative computation, to second order in the parameter $\alpha_S \mu / k_t$, of classical gluon radiation in nuclear collisions. We will then briefly discuss a non-perturbative Hamiltonian approach which suggests how all orders in $\alpha_S \mu / k_t$ can be computed numerically. The implementation of this approach on the lattice is described in section 3.

In high energy nuclear collisions, hard valence parton modes are highly Lorentz contracted, static sources of color charge for the wee Weizsäcker–Williams modes in the nuclei. The sources are described by the current

$$J^{\nu,a}(r_t) = \delta^{\nu+} g \rho_+^a(r_t) \delta(x^-) + \delta^{\nu-} g \rho_-^a(r_t) \delta(x^+), \quad (1)$$

where $\rho_{+,-}$ are the color charge densities of the hard modes. The classical field of the two nuclei is obtained by solving $D_\mu F^{\mu\nu} = J^\nu$ for the two above mentioned light cone sources.

Gluon distributions are simply related to the Fourier transform $A_i^a(k_t)$ of the classical field by $\langle A_i^a(k_t) A_i^a(k_t) \rangle_\rho$. The subscript ρ above refers to the averaging over the color charge distributions (performed independently for each nucleus) with the Gaussian weight μ^2 . We assume equal A for simplicity.

We have omitted the rapidity dependence of the charge distributions in the equations immediately above. The omission is discussed further in the next section. We note here that the rapidity dependence of the charge distribution is also absent in Ref. ¹⁵ (see the discussion below Eq. 3).

Before the nuclei collide ($t < 0$), a solution of the equations of motion is $A^\pm = 0$, $A^i = \theta(x^-)\theta(-x^+)\alpha_1^i(r_t) + \theta(x^+)\theta(-x^-)\alpha_2^i(r_t)$ where, ¹⁶

$$\alpha_{1,2}^i(r_t) = \frac{1}{ig} \left(P e^{-ig \int_{\pm\eta_{proj}}^0 d\eta' \frac{1}{\nabla_\perp^2} \rho_\pm(\eta', r_t)} \right)^\dagger \nabla^i \left(P e^{-ig \int_{\pm\eta_{proj}}^0 d\eta' \frac{1}{\nabla_\perp^2} \rho_\pm(\eta', r_t)} \right). \quad (2)$$

Above, $\eta = \eta_{proj} - \log(x^-/x_{proj}^-)$ is the rapidity of the nucleus moving along the positive light cone with the gluon field α_1^i and $\eta = -\eta_{proj} + \log(x_{proj}^+/x^+)$ is the rapidity of the nucleus moving along the negative light cone with the gluon field α_2^i . At central rapidities, (or $x \ll 1$) the source density varies slowly as a function of rapidity and $\alpha^i \equiv \alpha^i(r_t)$. The above expression suggests that for $t < 0$ the solution is simply the sum of two disconnected pure gauges. Just as in the Weizsäcker–Williams limit in QED, the transverse components of the electric field are highly singular.

For $t > 0$ the solution is no longer pure gauge. Working in the Schwinger gauge $x^+A^- + x^-A^+ = 0$, the authors of Ref. ¹⁵ found that with the ansatz $A^\pm = \pm x^\pm \alpha(\tau, r_t)$, $A^i = \alpha_\perp^i(\tau, r_t)$, (where $\tau = \sqrt{2x^+x^-}$), the Yang–Mills equations could be written in the simpler form

$$\begin{aligned} \frac{1}{\tau^3} \partial_\tau \tau^3 \partial_\tau \alpha + [D_i, [D^i, \alpha]] &= 0, \\ \frac{1}{\tau} [D_i, \partial_\tau \alpha_\perp^i] + ig\tau [\alpha, \partial_\tau \alpha] &= 0, \\ \frac{1}{\tau} \partial_\tau \tau \partial_\tau \alpha_\perp^i - ig\tau^2 [\alpha, [D^i, \alpha]] - [D^j, F^{ji}] &= 0. \end{aligned} \quad (3)$$

Note that the above equations of motion are independent of η —the gauge fields in the forward light cone are therefore only functions of τ and r_t and are explicitly boost invariant.

The initial conditions for the fields $\alpha(\tau, r_t)$ and α_\perp^i at $\tau = 0$ are obtained by matching the equations of motion at the point $x^\pm = 0$ and along the boundaries $x^+ = 0, x^- > 0$ and $x^- = 0, x^+ > 0$. Because the sources are highly singular functions along their respective light cones, so too in general

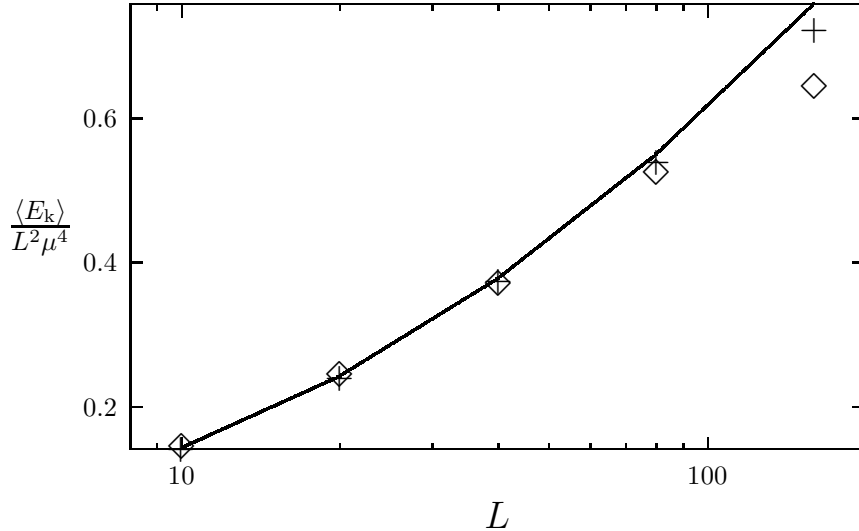


Figure 1: The lattice size dependence of the scalar kinetic energy density, expressed in units of μ^4 for $\mu = 0.025$ (pluses) and $\mu = 0.05$ (diamonds). The solid line is the LPT prediction. The error bars are smaller than the plotting symbols.

will be the equations of motion. Remarkably, there exist a set of non-singular initial conditions for the smooth evolution of the classical fields in the forward light cone. In terms of the fields of each of the nuclei before the collision ($t < 0$), they are, $\alpha_{\perp}^i|_{\tau=0} = \alpha_1^i + \alpha_2^i$ and $\alpha|_{\tau=0} = \frac{ig}{2}[\alpha_1^i, \alpha_2^i]$. Gyulassy and McLerran have shown¹⁶ that even when $\alpha_{1,2}^i$ are smeared out in rapidity to properly account for singular contact terms in the equations of motion, the above boundary conditions remain unchanged. Further, since the equations are very singular at $\tau = 0$, the only condition on the derivatives of the fields that leads to regular solutions are $\partial_{\tau}\alpha|_{\tau=0}, \partial_{\tau}\alpha_{\perp}^i|_{\tau=0} = 0$.

In Ref.¹⁵, perturbative solutions (for small ρ) were found to order ρ^2 by expanding the initial conditions and the fields in powers ρ (or equivalently, in powers of $\alpha_S\mu/k_t$) as $\alpha = \sum_{n=0}^{\infty} \alpha_{(n)}$; $\alpha_{\perp}^i = \sum_{n=0}^{\infty} \alpha_{\perp(n)}^i$. The subscript n denotes the n th order in ρ . For details of the perturbative solution, we refer the reader to their paper (see also the related paper of Gyulassy and McLerran¹⁶).

The perturbative Yang-Mills result for the number distribution of classical gluons is

$$\frac{dN}{dyd^2k_t} = \pi R^2 \frac{2g^6\mu^4}{(2\pi)^4} \frac{N_c(N_c^2 - 1)}{k_t^4} L(k_t, \lambda), \quad (4)$$

where $L(k_t, \lambda)$ is an infrared divergent function at the scale λ . We first note that this result agrees with the quantum bremsstrahlung formula of Gunion and Bertsch²⁰ and with several later works^{16,17,18}. It was also shown by Gyulassy and McLerran that for sources smeared out in rapidity, the resulting expression is identical to the one above except $\mu^4 \rightarrow \chi^+(y)\chi^-(y)$. The \pm superscripts refer to the nucleus on the positive or negative light cone respectively.

The origin of the infrared divergent function $L(k_t, \lambda)$ above is from long range color correlations that are cut-off either by a nuclear form factor (as in Refs.^{20,17}), by dynamical screening effects^{30,29} or in the classical Yang–Mills case of Ref.¹⁵, non-linearities that become large at the scale $k_t \sim \alpha_S \mu$. In the classical case then, $L(k_t, \lambda) = \log(k_t^2/\lambda^2)$ where $\lambda = \alpha_S \mu$. At sufficiently high energies, the behaviour of gluon radiation infrared is given by higher order (in $\alpha_S \mu/k_t$) non-linear terms in the classical effective theory.

It is unlikely that a simple analytical solution exists for the Yang–Mills equations in general. The classical solutions then have to be determined numerically for $t > 0$. The straightforward procedure would be to discretize the Yang–Mills equations but it will be more convenient for our purposes to construct the lattice Hamiltonian and obtain the lattice equations of motion from Hamilton’s equations. This will be done in the next section. Before we do that, we will discuss here the form of the continuum Hamiltonian.

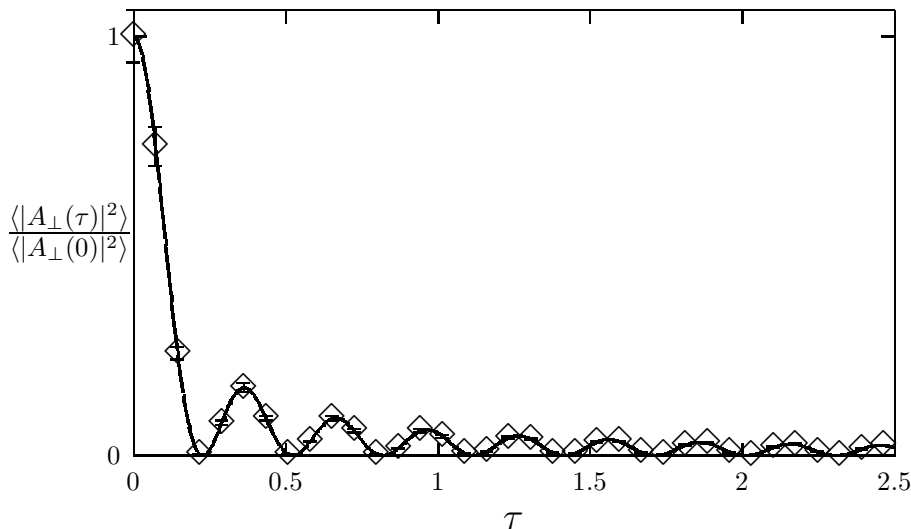


Figure 2: Normalized field intensity of a hard ($k_t = 2.16\text{GeV}$) mode vs proper time τ in units of fm (diamonds). Solid line is the LPTh prediction.

We start from the QCD action (without dynamical quarks) In the forward light cone ($t > 0$) it is convenient to work with the τ, η, \vec{r}_t co-ordinates where $\tau = \sqrt{2x^+x^-}$ is the proper time, $\eta = \frac{1}{2} \log(x^+/x^-)$ is the space-time rapidity and $\vec{r}_t = (x, y)$ are the two transverse Euclidean co-ordinates. In these co-ordinates, the metric is diagonal with $g^{\tau\tau} = -g^{xx} = -g^{yy} = 1$ and $g^{\eta\eta} = -1/\tau^2$.

After a little algebra, the Hamiltonian can be written as³¹

$$H = \int d\eta d\vec{r}_t \tau \left\{ \frac{1}{2} p^\eta p^\eta + \frac{1}{2\tau^2} p^r p^r + \frac{1}{2\tau^2} F_{\eta r} F_{\eta r} + \frac{1}{4} F_{xy} F_{xy} + j^\eta A_\eta + j^r A_r \right\}. \quad (5)$$

Here we have adopted the Schwinger gauge condition which is equivalent to requiring $A^\tau = 0$. Also, $p^\eta = \frac{1}{\tau} \partial_\tau A_\eta$ and $p^r = \tau \partial_r A_r$ are the conjugate momenta.

Consider the field strength $F_{\eta r}$ in the above Hamiltonian. If we assume approximate boost invariance, or $A_r(\tau, \eta, \vec{r}_t) \approx A_r(\tau, \vec{r}_t)$; $A_\eta(\tau, \eta, \vec{r}_t) \approx \Phi(\tau, \vec{r}_t)$, we obtain $F_{\eta r}^a = -D_r \Phi^a$. Here $D_r = \partial_r - ig A_r$ is the covariant derivative. Further, if we express $j^{\eta, r}$ in terms of the j^\pm defined in Eq. 1 we obtain the result that $j^{\eta, r} = 0$ for $\tau > 0$. Finally, since $\Phi = \tau^2 \alpha(\tau, \vec{r}_t)$; $A_r = \alpha_\perp^r(\tau, \vec{r}_t)$, we can perform the integration over the space-time rapidity to re-write the Hamiltonian in Eq. 5 as

$$H = \int d\vec{r}_t \tau \eta \left\{ \frac{1}{2} \left(\frac{\partial \alpha_\perp^r}{\partial \tau} \right)^2 + \frac{1}{4} F_{xy}^a F_{xy}^a + \frac{1}{2\tau^2} (D_\beta [\tau^2 \alpha])^2 \right\}. \quad (6)$$

Here the index $\beta = (\tau, \vec{r}_t)$. The discrete version of the above Hamiltonian is the Kogut-Susskind Hamiltonian³² in 2+1-dimensions coupled to an adjoint scalar field. The lattice Hamiltonian will be discussed further in the next section.

We now briefly comment on a key assumption in the above derivation, namely, the boost invariance of the fields. This invariance results in Eq. 6 thereby allowing us to restrict ourselves to a transverse lattice alone. There has been some confusion about the importance of boost invariance as a consequence of the initial assumption that the classical currents are delta functions on the light cone. For remarks clarifying this issue, see ref. ^{21,22}. In general, at the energies of interest, particle distributions are unlikely to be boost invariant⁶.

3 Real time lattice description of nuclear collisions

In this section, we discuss the problem on nuclear collisions on the lattice. Taking the naive continuum limit in the longitudinal directions of the full 4

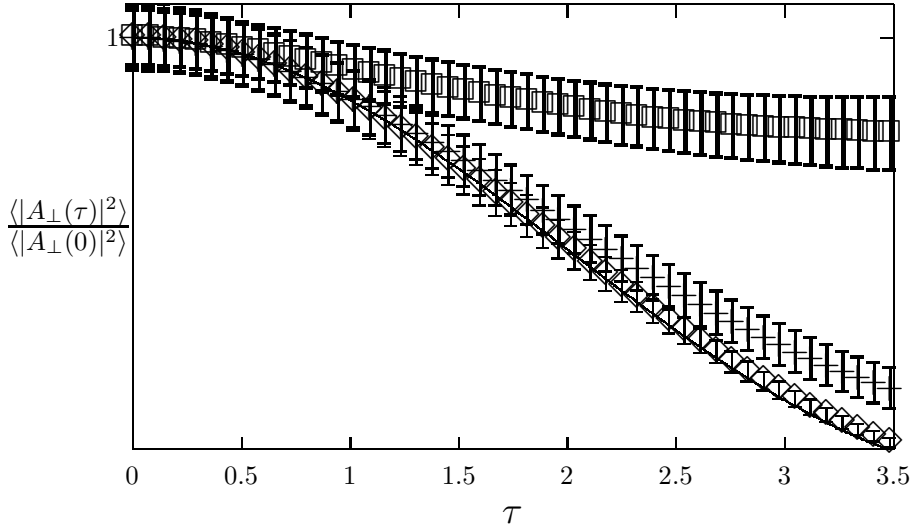


Figure 3: Normalized field intensity of a soft ($k_t = 108\text{MeV}$) mode vs proper time τ (in units of fm) for $\mu = 200\text{MeV}$ (squares), $\mu = 100\text{MeV}$ (pluses), and $\mu = 50\text{MeV}$ (diamonds). Solid line, nearly coinciding with the $\mu = 50\text{MeV}$ curve, is the LPT prediction.

dimensional Minkowski Wilson action for the $SU(N_c)$ gauge group in fundamental representation, one obtains an expression for the action S , which is discrete in the transverse directions and continuous in the z - t directions²². The equation of motion for a field is obtained by varying S with respect to that field. Initial conditions on the lattice are derived from the lattice analogue of the continuum initial conditions. We start from the lattice action S , obtain the lattice equations of motion in the four light cone regions and determine non-singular initial conditions by matching at $\tau = 0$ the coefficients of the most singular terms in the equations of motion. The full derivation is described in Ref.²².

The initial condition (at $\tau = 0$) for the transverse link field for the $SU(2)$ case is

$$U = \frac{\text{Tr}(U_1 + U_2)}{U_1^\dagger + U_2^\dagger} - I = (U_1 + U_2)(U_1^\dagger + U_2^\dagger)^{-1}. \quad (7)$$

For $N_c > 2$ the solution for U is not as simple. This condition has the right formal continuum limit. This can be seen by writing $U_{1,2}$ as $\exp(ia_{\perp}\alpha_{1,2})$ and U as $\exp(ia_{\perp}\alpha_{\perp})$. One obtains $\alpha_{\perp} = \alpha_1 + \alpha_2$ as required.

The result for the rapidity component of the gauge field (recall that we

had $A^\pm = \pm x^\pm \alpha(x_t, \tau)$ is

$$\begin{aligned} \alpha_\gamma = \frac{i}{4N_c} \sum_n \text{Tr} \sigma_\gamma \left([(U_1 - U_2)(U^\dagger - I) - \text{h.c.}]_{j,n} \right. \\ \left. - [(U^\dagger - I)(U_1 - U_2) - \text{h.c.}]_{j-n,n} \right). \end{aligned} \quad (8)$$

As above, in the limit of smooth fields, one obtains as required $\alpha = i \sum_n [\alpha_1, \alpha_2]_n$.

The lattice Hamiltonian is obtained from the action following the standard Kogut-Susskind procedure³², giving

$$\begin{aligned} H_L = \frac{1}{2\tau} \sum_{l \equiv (j,n)} E_l^a E_l^a + \tau \sum_{\square} \left(1 - \frac{1}{2} \text{Tr} U_{\square} \right), \\ + \frac{1}{4\tau} \sum_{j,n} \text{Tr} \left(\Phi_j - U_{j,n} \Phi_{j+n} U_{j,n}^\dagger \right)^2 + \frac{\tau}{4} \sum_j \text{Tr} p_j^2, \end{aligned} \quad (9)$$

where E_l are generators of right covariant derivatives on the group and $U_{j,n}$ is a component of the usual $SU(2)$ matrices corresponding to a link from the site j in the direction n . The first two terms correspond to the contributions to the Hamiltonian from the chromoelectric and chromomagnetic field strengths respectively. In the last equation $\Phi \equiv \Phi^a \sigma^a$ is the adjoint scalar field with its conjugate momentum $p \equiv p^a \sigma^a$. Matching the equations of motion at $\tau = 0$ gives us the initial conditions $E_l|_{\tau=0} = 0$, $\Phi_j|_{\tau=0} = 0$ and $p_j|_{\tau=0} = 2\alpha$.

Lattice equations of motion follow directly from H_L of Eq. 9. For any dynamical variable v with no explicit time dependence, $\dot{v} = \{H_L, v\}$, where \dot{v} is the derivative with respect to τ , and $\{\}$ denote Poisson brackets. We take E_l , U_l , p_j , and Φ_j as independent dynamical variables, whose only nonvanishing Poisson brackets are

$$\{p_i^a, \Phi_j^b\} = \delta_{ij} \delta_{ab}; \quad \{E_l^a, U_m\} = -i \delta_{lm} U_l \sigma^a; \quad \{E_l^a, E_m^b\} = 2\delta_{lm} \epsilon_{abc} E_l^c$$

(no summing of repeated indices). The equations of motion are consistent with a set of local constraints (Gauss' laws).

4 Mini-jets on the lattice: numerical results and comparison to lattice perturbation theory

In this section, we will compare results from our numerical simulations to analytic results from lattice perturbation theory. Before we do that we should first understand the ramifications of our results for nuclear collisions.

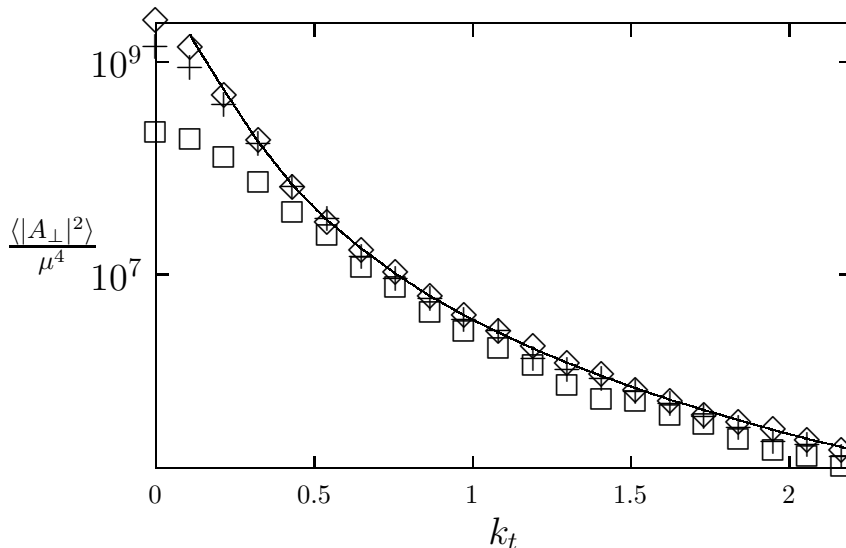


Figure 4: Field intensity over μ^4 as a function of k_t for $\mu = 200\text{MeV}$ (squares), $\mu = 100\text{MeV}$ (pluses), and $\mu = 50\text{MeV}$ (diamonds). Solid line is the LPTb prediction. The field intensity is in arbitrary units and k_t is in GeV.

In section 2, we introduced the scale μ^2 , which is the color charge squared per unit area. Its magnitude can be determined from the relation¹⁶

$$\mu^2 = \frac{A^{1/3}}{\pi r_0^2} \int_{x_0}^1 dx \left(\frac{1}{2N_c} q(x, Q^2) + \frac{N_c}{N_c^2 - 1} g(x, Q^2) \right), \quad (10)$$

where q, g stand for the *nucleon* quark and gluon structure functions at the resolution scale Q of the physical process of interest. Also, above $x_0 = Q/\sqrt{s}$. Using the HERA structure function data, Gyulassy and McLerran estimated that $\mu \leq 1$ GeV for LHC energies and $\mu \leq 0.5$ GeV at RHIC. Thus the regime where the classical Yang–Mills picture can be applied is rather limited. However, a window of applicability does exist and depending on what higher order calculations will tell us, this window may be larger or smaller than the naive classical estimates.

Gyulassy and McLerran¹⁶ have shown that the classical Yang–Mills formula in Eq. 4 is at small x (approximately) the same as the perturbative QCD prediction⁸ for the process $AA \rightarrow g$

$$\frac{d\sigma}{dy d^2k_t} = K_N \frac{\alpha_S N_c}{\pi^2 k_t^2} \int d^2q_t \frac{f(x_1, q_t^2) f(x_2, (\vec{k}_t - \vec{q}_t)^2)}{q_t^2 (\vec{k}_t - \vec{q}_t)^2}, \quad (11)$$

where $f(x, Q^2) = \frac{dxG(x, Q^2)}{d \log Q^2}$, and $x_1 \approx x_2 = k_t/\sqrt{s}$. The two formulae are equivalent if we divide the above formula by πR^2 , approximate the integral above by factoring out f above at the scale k_t^2 and taking the normalization factor $K_N \approx 5$.

At large transverse momenta, the field intensity measured on the lattice, $|A(k_t, \tau)|^2$, is simply related to the Yang–Mills distribution function. Then, from the above discussion, the field intensity of the hard modes on the lattice can also be simply related to the mini-jet cross section for the process $AA \rightarrow g$. However, at smaller transverse momenta, there is no simple relation between the field intensity and the classical gluon distribution function (and thereby the cross section by the above arguments). We have to look for more general quantities which, conversely, in the limit of large k_t , will give us the $AA \rightarrow g$ cross section. This point will be discussed further in Ref. ²².

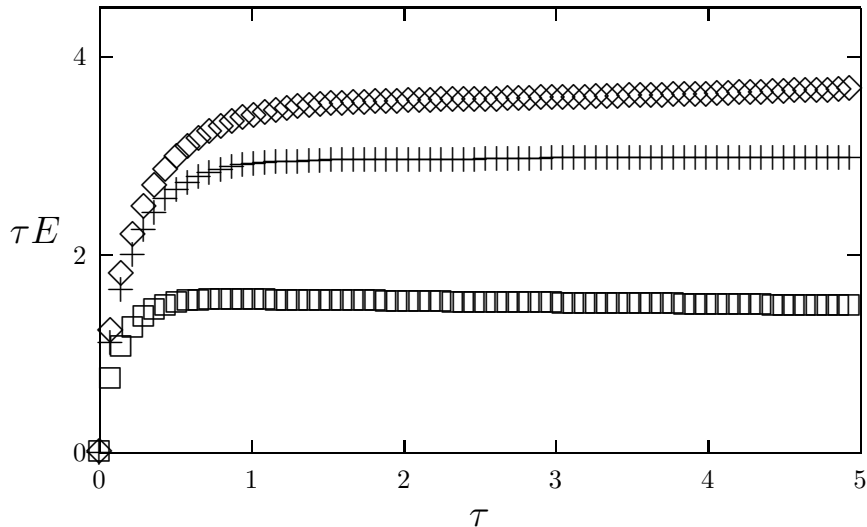


Figure 5: Time history of the energy density in units of μ^4 for $\mu = 200\text{MeV}$ (squares), $\mu = 100\text{MeV}$ (pluses), and $\mu = 50\text{MeV}$ (diamonds). Error bars are smaller than the plotting symbols. Proper time τ is in fm.

We now turn to numerical results from our simulations. These were performed for a variety of lattice sizes $L=20\text{--}160$ and the color charge density $\mu = 0.025\text{--}0.3$ in units of the lattice spacing a . To convert lattice results to physical units, we take $L^2 \approx \pi R^2$ for $A=200$ nuclei. This then also determines μ for a fixed lattice size. The relation of lattice time to continuum time is

given by the relation $\tau_C = a \cdot \tau_L$ ²³. In Fig. 1, we plot the Gaussian averaged initial kinetic energy $\langle E_k \rangle$ on the lattice as a function of the lattice size L and compare it with the lattice perturbation theory expression

$$p^a p^a = N_c(N_c^2 - 1) \left(\frac{\mu}{N}\right)^4 \quad (12)$$

$$\times \sum_{n,n'} \left[\left(\sum_l \frac{\sin(l_n) \sin(l_{n'})}{\Delta^2(l)} \right)^2 + 16 \left(\sum_l \frac{\sin^2(\frac{l_n}{2}) \sin^2(\frac{l_{n'}}{2})}{\Delta^2(l)} \right)^2 \right],$$

where $\Delta(l) = 2 \sum_n [2 - \cos(2\pi l_n/L)]$, $n = x, y$, and $1 - L/2 \leq l_{x,y} \leq L/2$. The comparison is made for values $\mu = 0.025, 0.05$ of the color charge density. For small values of L , there is very good agreement between the two but for the largest value $L = 160$, they begin to deviate. The strong coupling parameter on the lattice is $\propto g^2 \mu L$ ³³ and for $g^2 \mu L \gg 1$, we can expect to see deviations from lattice perturbation theory.

In Fig. 2, we plot the ratio of the field intensity of a particular mode of the transverse gauge field as a function of proper time τ normalized to its value at $\tau = 0$. The diamonds are results from a lattice simulation with $L = 160$ and $\mu = 0.025$ and the mode considered is $(k_x, k_y) = (\pi/4, 0)$. Note that $k_{x,y} = 2\pi l_{x,y}/L$ and for this case, $l_x = 20, l_y = 0$. The solid line in the figure is the square of the Bessel function $J_0(\omega\tau)$ where $\omega = \sqrt{\Delta(l)}$. The time dependence of the high transverse momentum modes should agree with the continuum perturbative result which predicts a time dependence proportional to $J_0^2(\omega\tau)$ for the field intensity of the transverse gauge fields. The continuum dispersion relation $\omega = |k_\perp|$ is however modified into the above mentioned lattice dispersion relation. We see from the figure that the anticipated agreement between the lattice results and perturbation theory is quite good.

In Fig. 3, we plot the same quantity as in Fig. 2, but now for three different values of μ and for the first non-zero momentum mode $(k_x, k_y) = (1, 0)$. The lattice size $L = 160$ is the same as previously. For the smallest value of $\mu = 0.025$, there is again an agreement with the Bessel behaviour predicted by perturbation theory. However at the larger values of $\mu = 0.05, 0.1$, one sees significant deviations away from the Bessel behaviour. Indeed the modes appear to saturate at larger values of τ . It is not clear that this saturation has much significance since the energy shows the expected $1/\tau$ behaviour at late times. The late time behaviour of long wavelengths may be understood better by looking at gauge invariant quantities²².

In Fig. 4, the field intensity of the transverse gauge field normalized by μ^4 at $\tau = 0$ is plotted as a function of the transverse momentum in physical units. The lattice results for the different values of μ described in the caption are

compared to the lattice perturbation theory result below for the field intensity (the prime denotes that α satisfies the Coulomb gauge condition):

$$|\alpha'_l|^2 = \frac{g^6 N_c (N_c^2 - 1) \mu^4}{4\Delta(l)} \sum_{l'} \frac{\Delta(2l' - l)\Delta(l) - [\Delta(l' - l) - \Delta(l')]^2}{\Delta^2(l')\Delta^2(l' - l)}. \quad (13)$$

The LPT_h result (which would be the mini-jet distribution in the continuum) agrees very well with the lattice result for small μ up to very small values of k_t . However, strong coupling effects grow with increasing μ (the lattice size L is fixed here) and we see deviations from the perturbative predictions at larger values of k_t . This trend is enhanced further at larger values of μ than those shown here. The non-perturbative effects due to the non-linearities in the Yang–Mills equations seem to temper the $1/k_t^4$ behaviour predicted by perturbation theory. Whether this reflects the presence of a time-dependent mass in the theory needs further investigation.

Finally, we plot the time dependence of the energy density for different values of μ . At late times, from general considerations we expect that $E \propto 1/\tau$ and that is indeed what we see. Perturbation theory predicts the energy densities will scale as μ^4 . Clearly our results do not show this scaling which suggests that non-perturbative effects are important. It appears though that the trend as we go to smaller values of μ is to approach the perturbative scaling behaviour.

5 Summary and outlook

In this paper, we have described results from real time lattice simulations of the full classical Yang–Mills equations with initial conditions given by the classical fields of each nucleus before the collision. At large transverse momenta, our simulations agree very well with lattice perturbation theory as they should. At small transverse momenta, we show that there are significant deviations from the LPT_h predictions. The late time behaviour of these modes is particularly interesting. The spatial dependence of equal time correlators provide further insight into these modes. These will be discussed in a forthcoming paper²². While this work was being prepared, we received a preprint studying lattice simulations of nuclei in a different approach³⁴.

Acknowledgments

We would like to thank the Universidade do Algarve (RV) and the Niels Bohr Institute (AK) for their kind hospitality. We would also like to thank Larry McLerran, Rob Pisarski and Dirk Rischke for very useful discussions. RV's

work is supported by the Danish Research Council and the Niels Bohr Institute. Both AK and RV acknowledge support provided by the Portuguese Fundação para a Ciência e a Tecnologia, grants CERN/S/FAE/1111/96 and CERN/P/FAE/1177/97.

References

1. See, for instance, the proceedings of *Quark Matter 96*, *Nucl. Phys. A* **610**, (1996).
2. K. Kajantie, P. V. Landshoff, and J. Lindfors, *Phys. Rev. Lett.* **59**, 2527 (1987);
K. J. Eskola, K. Kajantie, and J. Lindfors, *Nucl. Phys. B* **323**, 37 (1989);
J.-P. Blaizot and A. H. Mueller, *Nucl. Phys. B* **289**, 847 (1987).
3. X.-N. Wang, *Phys. Rep.* **280**, 287 (1997).
4. K. Geiger, *Phys. Rep.* **258**, 237 (1995).
5. M. Plumer, M. Gyulassy and X.-N. Wang, *Nucl. Phys. A* **590**, 511c (1995).
6. K. J. Eskola, K. Kajantie, and P. V. Ruuskanen, *Eur. Phys. J. C* **1**, 627 (1998);
K. J. Eskola, *Comments in Nucl. and Part. Phys.* **22**, 185 (1998).
7. R. Venugopalan, *Comments in Nucl. and Part. Physics* **22**, 113 (1998).
8. L. V. Gribov, E. M. Levin, and M. G. Ryskin, *Phys. Rep.* **100**, 1 (1983).
9. L. McLerran and R. Venugopalan, *PRD* **49**, 2233 (1994);
Phys. Rev. D **49**, 3352 (1994);
Phys. Rev. D **50**, 2225 (1994).
10. A. Ayala, J. Jalilian-Marian, L. McLerran and R. Venugopalan, *Phys. Rev. D* **52**, 2935 (1995);
Phys. Rev. D **53**, 458 (1996).
11. J. Jalilian-Marian, A. Kovner, L. McLerran and H. Weigert, *Phys. Rev. D* **55**, 5414 (1997).
12. J. Jalilian-Marian, A. Kovner, A. Leonidov and H. Weigert, *Nucl. Phys. B* **504**, 415 (1997);
hep-ph/9807462.
13. J. Jalilian-Marian, A. Kovner, and H. Weigert, hep-ph/9709432.
14. Yu. V. Kovchegov, *Phys. Rev. D* **54**, 5463 (1996);
Phys. Rev. D **55**, 5445 (1997).
15. A. Kovner, L. McLerran and H. Weigert, *Phys. Rev. D* **52**, 3809 (1995);
Phys. Rev. D **52**, 6231 (1995).
16. M. Gyulassy and L. McLerran, *Phys. Rev. C* **56**, 2219 (1997).
17. Y. V. Kovchegov and D. H. Rischke, *Phys. Rev. C* **56**, 1084 (1997).

18. S. G. Matinyan, B. Müller and D. H. Rischke, *Phys. Rev. C* **56**, 2191 (1997).
19. J. D. Bjorken, *Phys. Rev. D* **27**, 140 (1983);
J. Sollfrank, P. Houvinen, M. Kataja, P. V. Ruuskanen, M. Prakash and R. Venugopalan, *Phys. Rev. C* **55**, 392 (1997).
20. J. F. Gunion and G. Bertsch, *Phys. Rev. D* **25**, 746 (1982).
21. A. Krasnitz and R. Venugopalan, hep-ph/9706329, in proceedings of *3rd International Conference on the Physics and Astrophysics of the Quark Gluon Plasma*, March 17th–21st, Jaipur, India.
22. A. Krasnitz and R. Venugopalan, NBI-98-21, UALG/PT/5, to be published.
23. J. Ambjørn and A. Krasnitz, *Phys. Lett. B* **362**, 97 (1995);
Nucl. Phys. B **506**, 387 (1997).
24. G.D. Moore, *Nucl. Phys. B* **480**, 657 (1996).
25. A.H. Mueller, Y. Kovchegov, and S. Wallon, *Nucl. Phys. B* **507**, 367 (1997);
A. H. Mueller and Y. Kovchegov, hep-ph/9802440.
26. A.H. Mueller, *Nucl. Phys. B* **415**, 373 (1994).
27. A. Makhlin and E. Surdutovich, *Phys. Rev. C* **58**, 389 (1998).
28. I. Balitsky, hep-ph/9808215.
29. K. J. Eskola, B. Müller, and X.-N. Wang, *Phys. Lett. B* **374**, 20 (1996).
30. M. Gyulassy and X.-N. Wang, *Nucl. Phys. B* **420**, 583 (1994).
31. A. Makhlin, hep-ph/9608261.
32. J. Kogut and L. Susskind, *Phys. Rev. D* **11**, 395 (1975).
33. R. V. Gavai and R. Venugopalan, *Phys. Rev. D* **54**, 5795 (1996).
34. S. A. Bass, B. Müller and W. Pöschl, nucl-th/9808011.